THE ASTROPHYSICAL JOURNAL, 408:L109–L112, 1993 May 10

DETECTION OF H_3^+ INFRARED EMISSION LINES IN SATURN

T. R. GEBALLE
Joint Astronomy Center, 660 North A'ohōkū Place, University Park, Hilo, HI 96720

AND

M.-F. JAGOD AND T. OKA
Department of Astronomy and Astrophysics and Department of Chemistry,
University of Chicago, 5735 South Ellis Avenue, Chicago, IL 60637-1403
Received 1992 December 15; accepted 1993 February 23

ABSTRACT

Three emission lines of the ν_2 fundamental vibration-rotation band of H_3^+ have been detected in the ionosphere of Saturn near and at its poles. The peak observed column density of H_3^+ (at the south limb) is more than two orders of magnitude lower than the column density at the south pole of Jupiter and is less than that detected from Uranus. While the number and the signal-to-noise ratios of observed transitions are not sufficient to determine the temperature and abundance of H_3^+ accurately, the observed emission intensities are consistent with a temperature of ≈ 800 K and total column density of $\approx 1.0 \times 10^{11}$ cm^{-2}.

Subject headings: infrared: solar system — molecular processes — planets and satellites: individual (Saturn)

1. INTRODUCTION

The recent discovery of Jovian H_3^+ infrared emission in the 2 μm [$2\nu_2(2)$ overtone band] (Drossart et al. 1989; Trafton, Lester, & Thompson 1989) and in the 4 μm fundamental band (Oka & Geballe 1990; Miller, Joseph, & Tennyson 1990; Maillard et al. 1990) has provided planetary scientists with an important tool for monitoring ionospheric and auroral activity on that planet. The strength of the Jovian emission, particularly in the fundamental band suggested that the emission may be detectable in the more distant giant planets (Saturn, Uranus, and Neptune) which possess hydrogen-rich atmospheres.

We first attempted the detection of H_3^+ in Saturn at the United Kingdom Infrared Telescope (UKIRT) using its new 1–5 μm array grating spectrometer, CGS4, on 1991 July 20–21, without success (Geballe, Momose, & Oka, unpublished). The recent relatively easy detection by an improved CGS4 of H_3^+ line emission in Uranus (Trafton et al. 1993), line emission that was weaker than Jupiter's by almost two orders of magnitude, stimulated us to search again for the emission in Saturn in summer of 1992. We report the successful detection of H_3^+ in Saturn in this paper.

2. OBSERVATIONS

Spectra of Saturn were obtained by CGS4 at UKIRT on Mauna Kea during the nights of 1992 July 18 and 19 (UT). A 31 l/mm echelle and the 300 mm ("long") focal camera were employed in CGS4, along with a 58 × 62 array of InSb photodiodes. The resultant pixel dimensions on the sky were aproximately 1".1 × 2".2, with the smaller angle along the direction of the dispersion. The cold slit within CGS4, of width one pixel (1".1), was oriented along the polar axis of the planet. Unwanted orders of the echelle were blocked by a circular variable filter.

The observations of Saturn were made in a stare/nod mode. On the first night the nod position was blank sky adjacent to Saturn; on the second night the nod position was along the slit, placing Saturn's spectrum in rows of the array that had previously viewed sky. Flux calibration was achieved through observations of BS 7776, assumed to have an L-magnitude of 3.81 and a blackbody temperature of 6000 K. Seeing conditions were generally poor during both nights; as a result a significant portion of the stellar flux fell off of the slit and was not detected. An approximate correction for this was made during the flux calibration; however, the accuracy of the flux scale is probably only 30%. Wavelength calibration was obtained by a combination of observation of lines in arc lamps and from the wavelengths of telluric lines.

Two spectral intervals were chosen for study, one near 3.53 μm (2830 cm^{-1}), observed on July 18, and the second near 3.67 μm (2726 cm^{-1}), observed on July 19. Integration times were 80 minutes for the first interval and 132 minutes for the second. The first interval contains the $R(3, 3)^-(J = 4, G = 3, U = -1 \rightarrow J = 3, K = 3)$ transition at 2829.923 cm^{-1} (3.5337 μm) and five other transitions, all of which are seen in Jupiter. The second interval contains the close doublet, $R(1, 0)^+(J = 2, G = 0, U = +1 \rightarrow J = 1, K = 0)$ and $R(1, 1)^+$ $(J = 2, G = 1, U = +1 \rightarrow J = 1, K = 1)$, at 2725.898 and 2726.219 cm^{-1} (3.6685 and 3.6681 μm), respectively. These relatively short-wavelength fundamental band lines were selected in order to minimize the contribution to the spectrum by the reflected solar spectrum from the disk, which is strong at longer wavelengths and is severely complicated by gaps in the absorption from CH_4 in the atmosphere of Saturn. The resolution was 0.20 cm^{-1} at 2830 cm^{-1} and 0.17 cm^{-1} at 2726 cm^{-1}.

At the time of observation, the Saturnian disk had a polar diameter of 16".7, with the north pole 0".4 below the north limb and the south pole obscured. The disk was centered in one row of the array and was detected in four rows on either side of the central row. The filling factor for the outer rows was about 0.3. The rings occulted the disk well south of the equator; in the 3–4 μm band reflected solar radiation from the rings overwhelms the spectrum of the planet, from the central row through the row just above the south limb.

3. RESULTS

Figure 1 shows the spectrum in the 3.53 μm region at four locations on Saturn. The $R(3, 3)^-$ transition (2829.9 cm^{-1})

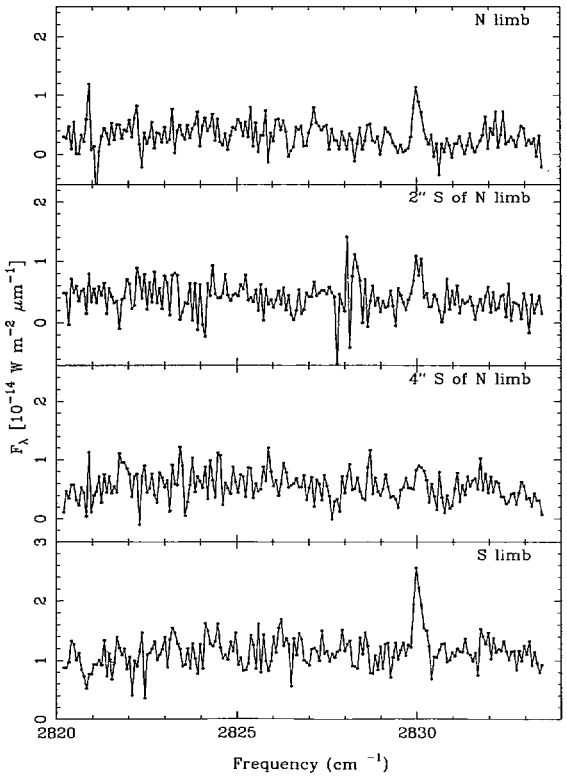

FIG. 1.—Spectra of four latitudes of Saturn in the 2830 cm^{-1} (3.54 μm) region. The emission line corresponds to the $R(3, 3)^-$ transition with the laboratory frequency of 2829.923 cm^{-1}. The $R(2, 1)^+$ transition at 2826.113 cm^{-1} is barely visible in the limbs. The uncertainty can be estimated from the scatter in the data points.

can be seen in each of the spectra. The line is strongest at the south limb. The line strength weakens going from the N limb toward the equator. Indeed, in the spectrum (not shown) roughly 6″ south of the N limb spectrum, the $R(3, 3)^-$ line is not detected. Below the equator the spectrum is severely contaminated by reflected radiation from the rings, except for the spectrum at the south limb.

The sum of the 3.53 μm spectra at the two limbs and that 2″ south of the north limb is shown in Figure 2, along with a spectrum of the south pole of Jupiter, obtained on 1992 July 17. Note the slight redshift of the Jovian spectrum relative to that of Saturn; this is due to the relative motions of the three planets. At the time of observation, the brightest H_3^+ line emission from Jupiter was at the south pole (shown). Thus the brightest H_3^+ line emission from Saturn was less intense than that from Jupiter by a factor of 130. The second strongest Jovian H_3^+ line in Figure 2 is the $R(2, 1)^+$ line at 2826.1 cm^{-1}. The line may be present marginally in the spectrum of Saturn, but the ratio of the two lines is 1/4 or less, whereas in Jupiter the ratio is 1/2. Theoretically the ratio should be $\approx 1/2.6$ over a wide range of assumed temperatures of the Jovian ionosphere. Thus the observed ratio is anomalously high in Jupiter and low in Saturn. The anomaly in Jupiter was also pointed out by Maillard et al. (1990) who noted that the intensity of the $R(3, 3)^-$ line is consistently low compared to many other lines and suggested atmospheric interference as its cause. Since the signal-to-noise ratio of the Saturn spectrum is low, further observation is required to establish the Saturnian anomaly. None of the other lines seen in this spectrum of Jupiter are apparent in the spectrum of Saturn.

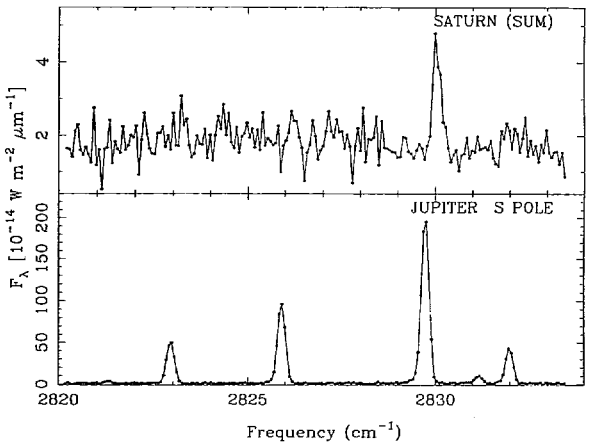

FIG. 2.—Combined spectrum of Saturn (the sum of panels 1, 2, and 4 in Fig. 1) in the 2830 cm^{-1} interval, along with a spectrum of the south pole of Jupiter. The Jupiter emission lines and their laboratory wavenumbers are (in descending order): $R(3, 2)^-$ 2832.197 cm^{-1}, $R(3, 1)^-$2831.340 cm^{-1}, $R(3, 3)^-$ 2829.923 cm^{-1}, $R(2, 1)^+$ 2826.113 cm^{-1}, $R(2, 2)^+$ 2823.138 cm^{-1} of the fundamental ν_2 band and $R(8, 9)$ of the $2\nu_2(0) \rightarrow \nu_2$ hot band.

Figure 3 shows a portion of the spectral region observed near 3.67 μm. The $R(1, 0)^+$ and $R(1, 1)^+$ doublet, at 2726 cm^{-1}, spaced by 0.32 cm^{-1} (35 km s^{-1}) is detected and resolved in the spectra of the north and south limbs as well as in the spectrum just south of the north limb. The strong emission features at $\approx$2724 and at $\approx$2730 cm^{-1} in these spectra apparently are gaps between strong and highly pressure-broadened absorption lines of methane in the atmosphere of Saturn. A weak and narrow feature near the doublet is seen in the north-

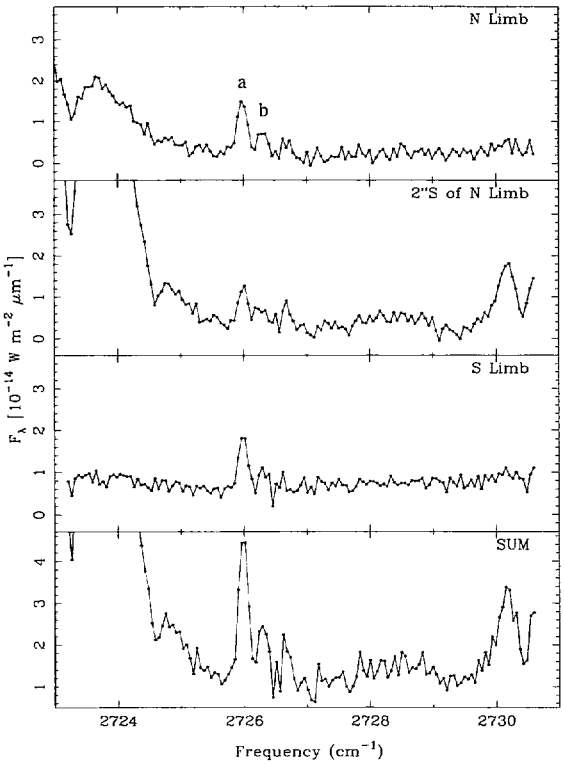

FIG. 3.—Spectra of three locations on Saturn, near 2726 cm^{-1} (3.67 μm). Line *a* is $R(1, 0)^+$ 2725.898 cm^{-1}, and line *b* is $R(1, 1)^+$ 2726.219 cm^{-1}.

ern spectra at about 2726.7 cm^{-1}. We suspect that this is a narrow gap between absorption features, rather than an emission line, as its strength appears to scale aproximately with the strength of the emission at the edges of the spectrum.

Observed intensities of the emission lines in the north and south limbs of Saturn are listed in Table 1 together with their assignment, laboratory wavenumbers ν_{lab} (cm^{-1}), spin statistical weight g_I, transition strength S, and the absolute energy values of the upper state of the transition E' (cm^{-1}).

4. DISCUSSION

4.1. *Physical Conditions and Abundance*

In principle the observed intensities listed in Table 1 should allow the temperature of H_3^+ to be determined for the north limb and south limb separately using the proportionality

$$I \sim g_I S \nu^3 \exp\left(\frac{-E'}{kT}\right).$$

In practice, however, the accuracy of the temperature determination is lowered by (a) large uncertainty of the observed intensities due to limited signal-to-noise ratio of the emission lines, (b) small differences in the values of E' due to low values of J, (c) the large time separation (i.e., rotation of the planet) between the measurements at 2830 and 2760 cm^{-1}, and (d) the likely different beam-filling factors at the two limbs during the two measurements. Using the observed intensities of the $R(3, 3)^-$ and $R(1, 0)^+$ transitions, we obtain $T = 570$ K for the north limb and $T = 1100$ K for the south limb with large uncertainties, especially for the latter. Assuming the temperatures of the two limbs to be equal and taking the average intensities, we obtain the temperature $T = 780$ K. This value is in accord with $T = 800$ K at and beyond 1540 km estimated by Festou & Atreya (1982) from the H_2 occultation measurements using the *Voyager 2* ultraviolet spectrometer.

The total column density nL of H_3^+ can be estimated from the photon counting formula

$$\frac{I}{h\nu} = \frac{\sigma}{4\pi} A_{ij} nL f_{vr},$$

where I is the observed emission intensity (W m^{-2}), σ is the beam size (radian^2), A_{ij} is the Einstein coefficient for spontaneous emission (s^{-1}), and f_{vr} is the fraction of H_3^+ in the emitting vibration-rotation level. Using the observed emission intensity $I = \int I_{obs}\, d\lambda = 3.4 \times 10^{-18}$ W m^{-2}, the beam size $\sigma = 1''.1 \times 0''.68 = 1.68 \times 10^{-11} \times 10^{-11}$ (allowing for the underfilling of the limbs), and the Einstein coefficient of 60.4 s^{-1} (Kao et al. 1991), we calculate the column density of H_3^+ in the $\nu_2\, J = 2$, $G = 0$, $U = +1$ level to be 7.9×10^7 cm^{-2}, and the column density of H_3^+ in the ν_2 state to be 2.3×10^9 cm^{-2}. The estimate of the total column density depends critically on the temperature. If we assume the rovibrational distribution of H_3^+ to be thermal with $T = 800$ K, we find $f_{vr} = 7.5 \times 10^{-4}$ and the total column density of H_3^+ is $nL = 1.0 \times 10^{11}$ cm^{-2}. The total column density is lower if the temperature is higher than the assumed temperature of 800 K and vice versa. Atreya et al. (1983) calculated a chemical model of the Saturnian ionosphere and reported the H_3^+ number density to be 10–80 cm^{-3} between the altitudes of 3500 and 1000 km and that the number density increases to $\approx$2000 cm^{-3} at the thin layer around 1000 km (Fig. 16 of Atreya et al. 1983). Their total column density of $\sim 10^{10}$ cm^{-2} is smaller than our value by about one order of magnitude. Limb brightening may well account for much or all of the discrepancy.

The calculated intensities for the emission lines based on the total column density of 1.0×10^{11} cm^{-2} and temperature of 800 K are given in the last column of Table 1. They are in general agreement with observed values within the uncertainty of observation.

4.2. *Morphology*

In some respects the distribution of H_3^+ line intensities on Saturn appears similar to that on Jupiter. In our 1992 July observation of Jupiter (Geballe, Jagod, & Oka, unpublished), the observed intensities of the H_3^+ emissions at the north pole were lower by a factor of about 3 and higher than those near the equator by an order of magnitude. By comparison, the intensities at the north and south limbs of Saturn were roughly the same, and a drop-off of about a factor of 3 was seen on Saturn 4″ south of its north limb (Fig. 1). The drop-off appears less abrupt on Saturn than on Jupiter. However, the line intensities at Saturn's equator cannot be determined. Moreover, the observed differences between the two in their northern hemispheres are almost certainly strongly affected not only by the small beam-filling factor at the north limb of Saturn, but also by the pixels covering about twice the surface area on Saturn than on Jupiter (due to their different distances from Earth). Both of these effects tend to diminish the contrast on Saturn.

The H_3^+ line intensities observed by us at the Jovian south pole were roughly 3 times greater than at its north pole (Geballe, Jagod, & Oka, unpublished), whereas the line intensities at Saturn's south limb were roughly comparable to those

TABLE 1

OBSERVED H_3^+ EMISSION LINES

Transition $JGU \rightarrow JK$	Laboratory Wavenumbers ν_{lab} (cm^{-1})	Spin Weight g_I	Transition Strength S	Emitting Energy Level E' (cm^{-1})	Limbs	I_{obs}[a]	Calculated Flux I_{calc}[a]
4 3 −1 3 3 $R(3, 3)^-$	2829.923[b]	4	0.1340	3145.275	N	2.5 ± 0.5	3.4
					S	4.5 ± 0.5	3.4
2 1 +1 1 1 $R(1, 1)^+$	2726.219[c]	2	0.0474	2790.346	N	1.2 ± 0.4	1.1
					S	1.1 ± 0.4	1.1
2 0 +1 1 0 $R(1, 0)^+$	2725.898[c]	4	0.0777	2812.861	N	3.4 ± 0.4	3.6
					S	3.0 ± 0.4	3.6

[a] In units of 10^{-18} W m^{-2}.

[b] Observation date UT 1992 July 18 1400–1600 hr.

[c] Observation date UT 1992 July 19 1300–1600 hr.

at the north pole (Figs. 1 and 3). However, filling factors (uncertain, and probably different) at the north and south limbs and the obscuration of Saturn's south pole behind the limb of the planet certainly affect the observations of Saturn.

It could well be that the distributions of H_3^+ line emission on the two planets are quite similar, although it is still possible that the distribution on Saturn may be explainable in terms of the limb-brightening of a uniform distribution of H_3^+. Given the paucity of data, especially the lack of spectra near the central equator, the uncertainty in the amount of underfilling at the limbs of Saturn, and the low angular resolution of the present measurements, any conclusions at this time are premature.

4.3. *Comparison of the Three Planets*

Saturn is the third object and the third planet, after Jupiter and Uranus, for which H_3^+ line emission has been detected. The strongest line detected from Saturn is the $R(3, 3)^-$ line in the spectrum at the south limb (Fig. 1, *bottom panel*); its flux is 3.5×10^{-18} W m^{-2}. Comparison of the spectra of Jupiter and Saturn indicates that the peak H_3^+ line emission intensities in the two planets differ by about two orders of magnitude. Measurements of Uranian H_3^+ line emission made during this observing run indicate that the line emission from Saturn is a few times weaker than that from Uranus, and are consistent with the finding of Trafton et al. (1993) that the H_3^+ line intensity from Uranus is a few percent of that from Jupiter. The upper limits of 5×10^{-18} W m^{-2} for H_3^+ line fluxes from Neptune in a 3".1 square aperture (Trafton et al. 1993) are several times greater than the typical H_3^+ line strengths detected from Saturn in the present experiment in which a pixel subtends $\frac{1}{4}$ of the solid angle as it did in the Neptune experiment.

Trafton et al. (1993) already have considered the apparent puzzle of Uranus' H_3^+ emission being stronger than that of Saturn. They point out that the observed H_3^+ emission from Uranus implies a much higher rate of energy deposition (and perhaps H_3^+ production) than had been deduced from early *Voyager* measurements, which suggests that Uranus H_3^+ emissions might have been unusually bright when first detected. However, our measurements of Uranus in 1992 July indicate little change in the intensity of H_3^+ line emission. The ratio of Uranian and Jovian disk-average H_3^+ emissions is roughly the inverse of the square of the ratio of their distances from the Sun. Thus, the puzzle could be that Saturn's emissions are anomalously weak. Trafton et al. also considered this and suggest that it could be due to the more rapid destruction of H_3^+ by hydrocarbons in Saturn's upper atmosphere than in Jupiter or Uranus.

Until more observation of H_3^+ in Jupiter, Saturn, and Uranus are made, the normal abundances of H_3^+ in these planets will be uncertain, and it will be possible only to speculate on the detailed mechanisms that produce, excite, and destroy H_3^+ in them. In all likelihood, the H_3^+ ions are produced in planetary ionospheres through ionization of H_2, followed by the ion-neutral reaction

$$H_2^+ + H_2 \rightarrow H_3^+ + H \, .$$

The latter process is so efficient than the rate-determining process of the production of H_3^+ must be the ionization. The H_3^+ ions are destroyed by electron recombination or by proton hop reactions with other neutral molecules such as CH_4. This latter process may be dominant at a lower altitude of $\approx$1000 km as demonstrated by the abundance of CH_5^+ calculated by Atreya et al. (1983). However, at higher altitude, the electron recombination dominates.

Equating the production and destruction mechanisms of H_3^+, we have

$$\zeta[H_2] = k[H_3^+][e] \, ,$$

where k is the recombination rate constant (cm^3 s^{-1}) and ζ is the ionization flux (s^{-1}). If we use our value of $[H_3^+] \approx 500$ cm^{-3} [obtained from the total column density of 1×10^{11} cm^{-2} and assumed thickness of 2000 km (Atreya et al. 1983)], the reported value of $[e] \sim 10^4$ cm^{-3} by Tyler et al. (1981), and the rate constant of 10^{-7} cm^3 s^{-1} (Amano 1990; Canosa et al. 1992), we find the ionization rate of $\approx$0.5 cm^{-3} s^{-1} in Saturn. Whether this ionization is due to the local plasmas, to the solar wind or to photoionization remains to be seen. In Jovian polar regions the values of $[H_3^+]$ and $[e]$ are greater by at least two orders of magnitude and one order of magnitude, respectively, than in Saturn, and the ionization must be at least three orders of magnitude higher than in Saturn.

We are grateful to the staff of UKIRT for their support of this research. M.-F. J. and T. O. were supported by NSF grant PHY-90-22647. We thank the referee for several valuable comments.

REFERENCES

Amano, T. 1990, J. Chem. Phys., 92, 6492
Atreya, S. K., Waite, J. H., Jr., Donahue, T. M., Fagy, A. F., & McConnell, J. C. 1983, Saturn, ed. T. Gehrels & M. S. Mathews (Tucson: Univ. Arizona Press), 239
Canosa, A., Gomet, J. C., Rowe, B. R., Mitchell, J. B. A., & Queffelec, J. L. 1992, J. Chem. Phys., 97, 1028
Drossart, P., et al. 1989, Nature, 340, 539
Festou, M. C., & Atreya, S. K. 1982, Geophys. Res. Lett., 9, 1147
Kao, L., Oka, T., Miller, S., & Tennyson, J. 1991, ApJS, 77, 317
Maillard, J.-P., Drossart, P., Watson, J. K. G., Kim, S. J., & Caldwell, J. 1990, ApJ, 363, L37
Miller, S., Joseph, R. D., & Tennyson, J. 1990, ApJ, 360, L55
Oka, T., & Geballe, T. R. 1990, ApJ, 351, L53
Trafton, L. M., Geballe, T. R., Miller, S., Tennyson, J., & Ballester, G. E. 1993, ApJ, 405, 761
Trafton, L. M., Lester, D. F., & Thompson, K. L. 1989, ApJ, 343, L73
Tyler, G. L., Eshleman, V. R., Anderson, J. D., Levy, G. S., Lindel, G. F., Wood, G. E., & Croft, T. A. 1981, Science, 212, 201